Journal of Multidisciplinary Engineering Science Studies (JMESS)
ISSN: 2458-925X
Vol. 3 Issue 8, August - 2017

Thermal Simulation Analysis Of Battery Storage System For Hybrid Locomotive

Sarang Subhedar and Pradip Majumdar
Department of Mechanical Engineering
Northern Illinois University
DeKalb, Illinois, USA

David Schroeder and Rao Kilaparti
Department of Technology
Northern Illinois University
DeKalb, Illinois, USA

***Abstract*—The interest for developing hybrid electric locomotives consisting of diesel engine, regenerative braking and battery storage is growing due to increased demand and cost of diesel oil, uncertainty in the steady supply of oil, and increased standards for reduced emissions. Electrical energy is lost from electric locomotives in the form of heat during dynamic braking. Routing this energy using a regenerative braking system into battery stacks can improve the overall efficiency as it can be used later to provide traction force during acceleration. Objective of this study is to perform a feasibility analysis of modes of regenerating the energy developed in the braking and storing the energy in an electric battery storage system for use in road locomotive applications. Various road locomotive duty cycles, charge and discharge rates, and environmental conditions have been considered as this is expected to substantially influence the optimal performance and safety of the battery as well as the potential fuel savings that could be realized using a hybrid design. A computational algorithm is developed to determine the amount of energy that can be obtained from regenerative breaking during the run of locomotive and can be stored back into the stack of battery, which can be coupled with diesel engine to save additional consumption of fuel. A combined electrochemical and thermal simulation analysis of several battery configurations using multiphysics simulation code has also been performed in order to understand the thermal management and cooling requirements of the batteries subject to the charging and discharging requirements of a locomotive engine. Such an analysis assists in addressing the key issue of operating the battery at a maximum efficiency level while dissipating any excessive heat generated during the operation, and maintaining the battery at a desired temperature range using a cooling scheme.**

Keywords—Battery Storage, Simulation, Duty cycle

I. INTRODUCTION

The transportation sector is a major contributor to the greenhouse effect. To reduce this contribution, hybrid electric vehicles (HEV) and plug in hybrid electric vehicles (PHEV) have been introduced [1,5-6]. Outside of automobiles and trucks, diesel locomotives are the next largest consumer of transportation fuel in the US. Hybrid locomotives are being developed to reduce these emissions. Diesel locomotives typically have a much longer service life than automobiles, trucks, or airplanes, many have been in service since the 1960's. It is therefore important not just to consider the development of new hybrid diesel locomotives but also to consider the potential retrofit of existing locomotives. [2,5-7].

The operation of diesel electric locomotives is based on transfer of power from the engine to the wheels and is done via an electric generator and a traction motor. Hybrid locomotives basically use diesel and battery power during operation. There is a rechargeable energy storage system, which is installed between the power source and transmission system; this transmission system provides power to the wheels for propulsion. Most existing diesel locomotives are diesel electric and possess the basic components except the rechargeable energy storage system. Thus, the idea of a retrofit solution for hybrid locomotives does not seem unreasonable.

To reduce wear on friction brakes, diesel electric locomotives generally use their electric motors for braking converting energy into heat via large air cooled resistor banks. This dynamic braking energy can be utilized and stored in a rechargeable energy storage system. The dynamic braking takes the advantage of traction motor armatures, which are continuously rotated when the locomotive is running. The motor can be made into a generator which generates electric power that is supplied back to the rechargeable storage system.

The rechargeable energy storage system must be made up of many batteries connected in series and parallel to take the load of a locomotive. Generally, the locomotive runs at 600-3000V DC, so the storage system should be able to supply at least 600 V and sustain the further requirement [3]. To obtain the required voltage, batteries with high energy density and high power should be used. In today's market, there are various types of batteries, but of these Lithium-ion batteries are suggested to be promising in these kinds of applications.

The objective of this study is to design a battery energy storage system for a hybrid electric locomotive with diesel engines and regenerative braking. This helps to obtain improved fuel economy, reduced dependence on conventional fuel, and lower emissions of environmentally unsafe pollutants. Feasibility analysis is being performed considering different battery types, performance, capacity, power density, cost and considering road locomotive duty cycles as this influences the optimal performance of the battery as well as the potential fuel savings that could be realized using a hybrid diesel-battery storage design. Thermal management requirements of the locomotive battery energy storage system are also being examined using a computer simulation model under a range of ambient conditions which have influence on the operating temperature, performance and safety of the battery.

II. Duty Cycle Analysis

For the selection of the type of battery and size of a Battery Energy Storage System for locomotive engines, the propulsive energy requirement during the discharge mode and regenerative braking energy available during the charging mode of the battery were analyzed based on different real-world duty cycles of the locomotive engine. The duty cycle data for empty and loaded locomotive are analyzed to compare the amount of regeneration energy available in both the cases. These data included tractive force supplied by the engine to the traction motor, and the velocity of the locomotive with respect to time in seconds. Based on the data, calculations are performed for the power required by the traction motor and the available regenerative braking. Energy is given as a function of time and is based on the speed of the locomotive and the traction force requirement of the traction motor.
Figure 1, shows the energy distribution for both an empty locomotive and a loaded locomotive during the time the data were collected.

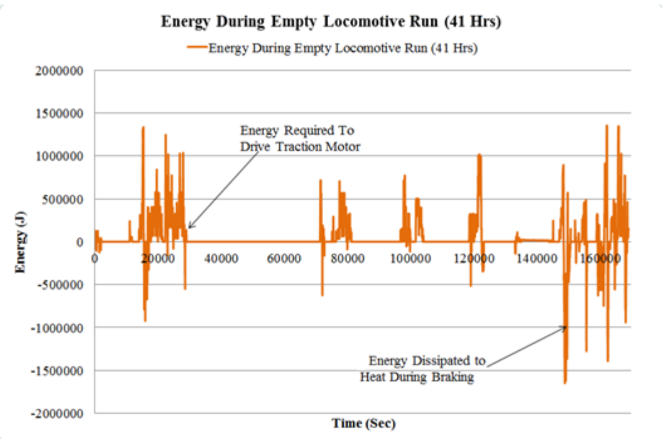

(a) Empty locomotive run

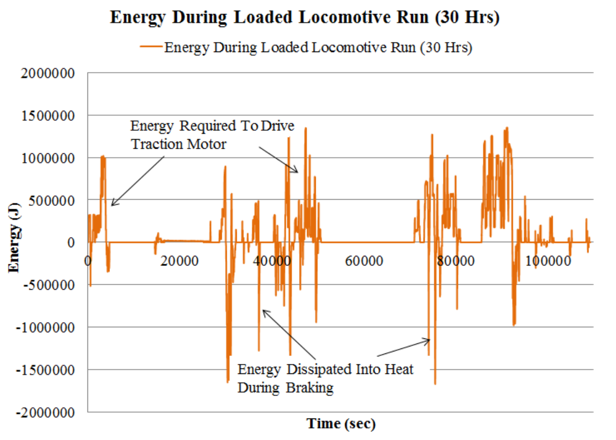

(b) Loaded locomotive run

Figure1 Energy distribution during locomotive run

Table 1 Summary of energy distribution

Engine duty cycle type	Run time (Hrs)	Total Energy Expended by Traction Motor (MJ)	Average rate of expended energy (MW)	Energy dissipated by resistive braking (MJ)	Average Rate of energy dissipated in brakes (MW)	Maximum available energy for battery storage (%)
Empty Locomotive	41	10,698	0.06322	2,939	0.01737	27.5
Loaded Locomotive	30	12, 673	0.11542	3,587	0.03267	28.3

Table 1 summarizes the energy use for the two duty cycles analyzed. The total amount of energy that is dissipated by the dynamic resistive braking is around 27.5% and 28.3% of the energy expended in traction for the empty and loaded engine respectively. In reality, only a fraction of this lost energy is recovered and utilized using a regenerative braking and battery energy storage system. To determine the amount of energy that can be captured, converted, and stored in BESS, a computer code was developed. This computer code takes into account the capacity of a battery at different C-rates for charging and discharging, battery state of charge (SOC), and data sets for energy expended by traction motor and energy dissipated in dynamic braking.

The voltage was calculated based on empirical equations obtained experimentally for the Valence Battery model # *U27-12XP* during discharge and charge [21]. These equations are used in the code to demonstrate the effect of voltage drop and rise in the BESS. As a test example, the Valence battery has been used in calculations and in the design of the battery stacks.

At discharge

Voltage = $-5E\text{-}07x^5 + 0.0001x^4 - 0.0101x^3 + 0.3665x^2 - 5.6438x + 671.35$

At charge

Voltage = (Voltage(i-1)+((2e-6x^4-0.003x^3 + 0.0163x^2 + 1.934x + 600.02) - 600)

In the above equations *x* represents the SOC. Combining the duty cycle data with the energy analysis of the duty cycle and the proposed battery pack, assuming that the battery pack is initially fully charged, yields results for state of charge over time shown in Figure 2. The results shown assume 5% of energy is lost as heat for both charge and discharge.

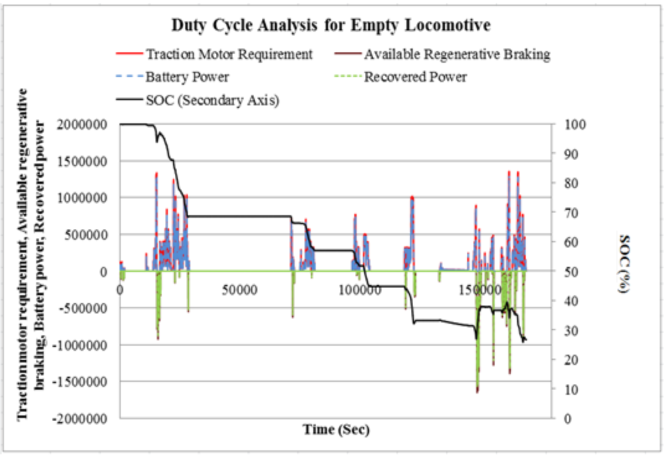

(a) Empty locomotive

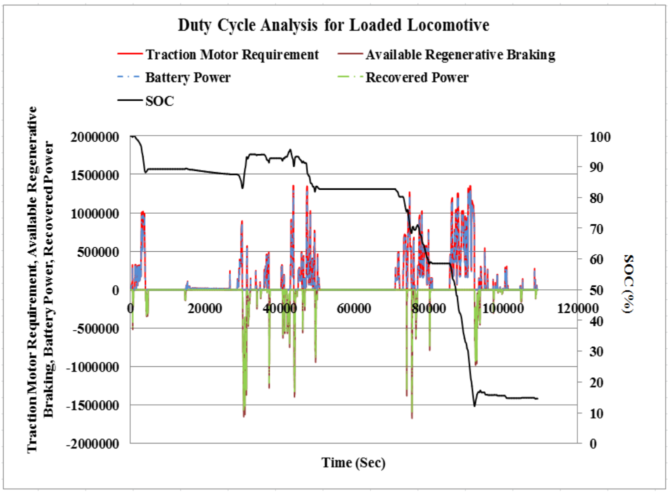

(b) Loaded locomotive

Figure 2. Duty cycle analysis for empty locomotive

Table 2 Duty cycle analysis results

Parameters	Loaded	Empty
SOC	$1x10^{10}$ J	$1x10^{10}$ J
Total Traction Motor Requirement	1.27 $x10^{10}$ J	1.07$x10^{10}$ J
Total Battery Energy	1.2$x10^{10}$ J	1.02 $x10^{10}$ J
Total Available Regenerative Braking	3.64$x10^9$ J	2.9 $x10^9$ J
Recovered Regenerative Braking	3.46$x10^9$ J	2.8 $x10^9$ J
% Recovered Regenerative Braking	27.20%	26.50%

III. ENERGY STORAGE SYSTEM MODELS COMPARISON

There are two types of BESS presented in this study. The first model is the Valence Batteries model # U27-12XP and other is the AA Portable Power Corp Model # PL-9759156-10C. The table below shows the stack wise relationship between the two models.

Table 3 Energy storage system model comparison

Type	Stack	Number of cells		Max. Voltage (V)	Max. Ampere (A)
		Series	Parallel		
Valence Model U27-12XP	50S19P	50	19	640	2622
AA Portable Power Corp. Model PL-9759156-10C	40S65P	40	65	640	2600

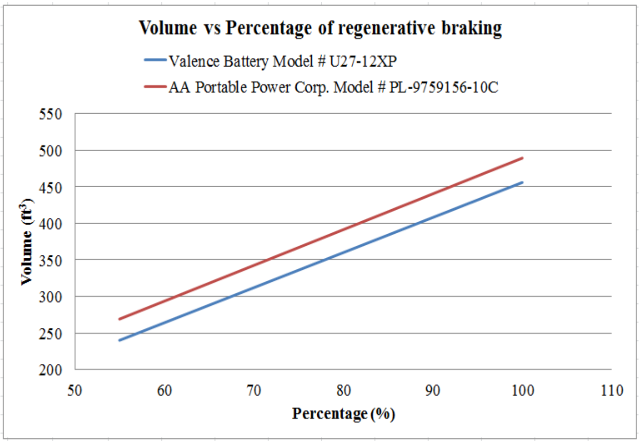

Figure 3 Volume comparison based on recovered regenerative braking

A comparative graph shown in Figure 3 displays the variation in the required volume of the battery storage system as a function of the percentage of peak regenerative energy to be stored. It can be observed that the required volume for the energy storage system increases linearly with the increase in percentage of peak energy to be stored. The volume required by the Valence battery is less compared to the volume required by the AA Portable Power battery model. The reason behind the high-volume requirement is the low single cell capacity.

IV. LOAD CYCLE ANALYSIS OF BATTERY

In this section, the load cycle data analysis process is discussed and a representative load cycle for a single cell is presented that is incorporated in the COMSOL multiphysics model in order to demonstrate the heat generation and its effects on the overall battery performance.

DEVELOPMENT OF LOAD CYCLE FOR BATTERY

As discussed in the earlier section the BESS is the base for generating the representative load cycle, the total number of battery packs in the stacks is 950. The battery type under consideration is U27-12XP. The battery packs internal construction contains 4 cells in series, each 3.2 volts and 138Ah. Using this information, a typical representative load cycle is constructed using the duty cycle data.

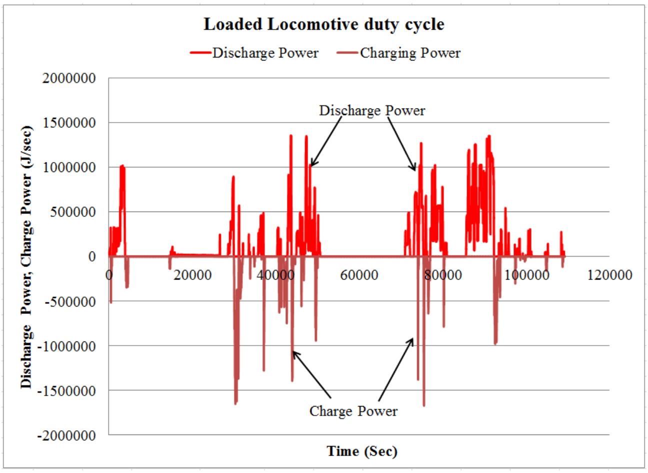

Figure 4. Loaded locomotive duty cycle

The process involves the reduction of power value from pack value to single cell value. The power that is available must be divided into the number of cells in the stack. For this study, the voltage is assumed to be constant. Based on performed calculations it can be concluded that the scaling factor (F_s) can be used to find the current during duty cycle. The current (A) is then plotted as a function of time and is shown in Figure 5.

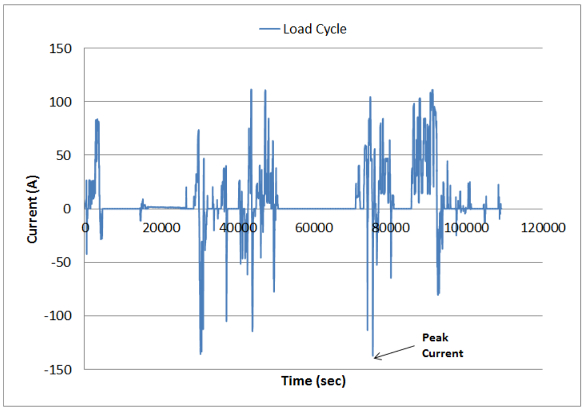

Figure 5 Load cycle showing current per cell

In the present simulation model, current density must be applied at the current collector tab. However, current density at the tab is different from current density at the frontal surface of the 2D battery. Finally, frontal current density is scaled down for tab current density based on area ratio. This is obtained as a product of current density of frontal surface and the ratio of the cell height to the collector thickness. For the COMSOL model, the calculated tab current density must be applied to the positive current collector. These current densities are scaled down with respect to the Valence battery energy storage system and shown below.

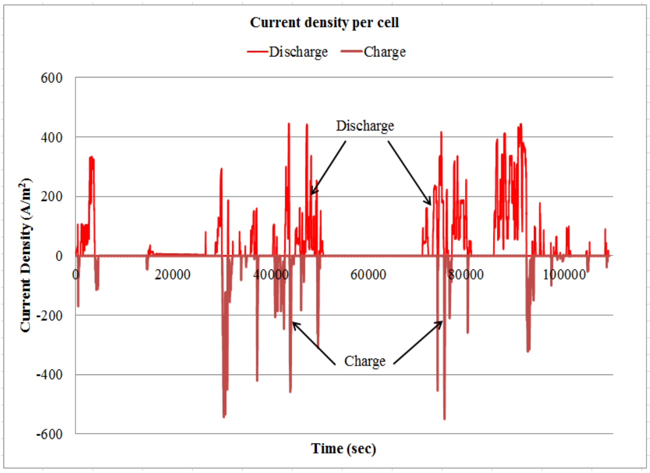

(a) Current density per cell

Journal of Multidisciplinary Engineering Science Studies (JMESS)
ISSN: 2458-925X
Vol. 3 Issue 8, August - 2017

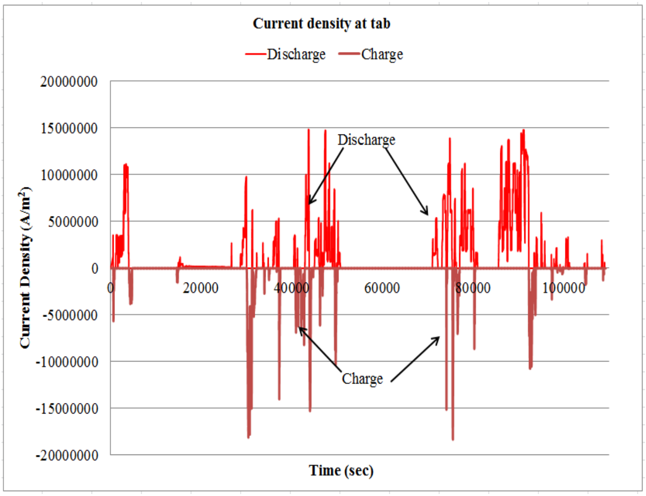

(b) Current density at the ta

Figure 6 Load cycle for simulation analysis of single battery cell

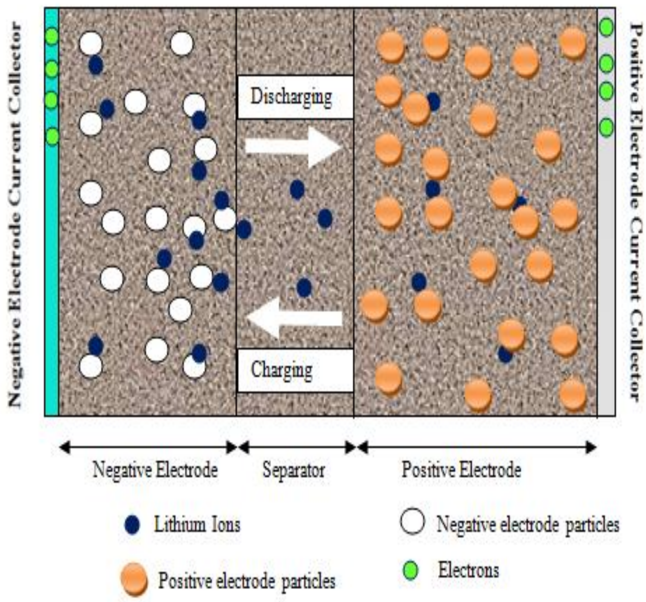

Figure 7 Schematic of battery model

Battery Simulation Model

A schematic of the lithium-ion battery considered in the current simulation model is shown in Figure – 1. The Battery cell consists of lithium porous manganese dioxide ($\boldsymbol{Li_yMn_2O_4}$) as the cathode, lithiated porous carbon ($\boldsymbol{Li_xC_6}$) as the anode and a separator, which gives stability to the model. The separator is a porous matrix that provides mechanical stability to the cell and is made of a copolymer of vinylidene fluoride and hexafluoropropylene (VdF-HFP). The pores of the negative electrode, separator, and positive electrode are filled with electrolyte. Electrolyte in this model consists of a mixture of ethylene carbonate (EC-$C_3H_4O_3$) and dimethyl carbonate (DMC-$C_3H_6O_3$) in a ratio of 1:2 of their volumes with lithium hexafluorophosphate ($LiPF_6$) as a salt. Finally, the negative current collector is made up of copper (Cu) and the positive current collector is made up of aluminum (Al).

The reactions involved during deintercalation and intercalation are as below.

Discharging

$$Li_xC_6 \rightarrow xLi^+ + xe^- + 6C$$
$$Li_yMn_2O_4 + xLi^+ + xe^- \rightarrow Li_{x+y}Mn_2O_4$$

Charging

$$xLi^+ + xe^- + Li_0C_6 \rightarrow Li_xC_6$$
$$Li_{x+y}Mn_2O_4 \rightarrow Li_yMn_2O_4 + xLi^+ + xe^-$$

A detail description of simulation model considered in this study is given by Bidawi et al. [4].

Partial Load Cycle

In the present study, a part of loaded locomotive engine load cycle is used for the thermal and electrochemical analysis of the battery simulation. The load cycle duration of 1800 seconds is considered and displayed in Figure 8 below. The load cycle takes into consideration the effect of the discharge, charge, and the open circuit. The time for each component of the load cycle consists of discharge as 1232 seconds, charge as 253 seconds and finally an open circuit as 315 seconds.

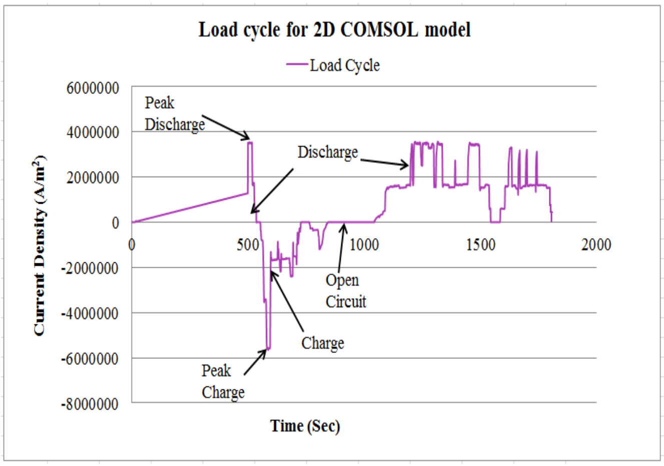

Figure 8 Load cycle for battery simulation model

V. Simulation Results

In this case the amount of regenerative braking that is recovered for two cases, 100% and 60% recovery, are compared. The complete recovery regenerative braking is actually not possible but in this case, it will help to understand the effect of amount of temperature rise in the battery. The 60% case is considered to support the conclusion for the BESS. Results show contour plot at the end of the load cycle at 1800th second.

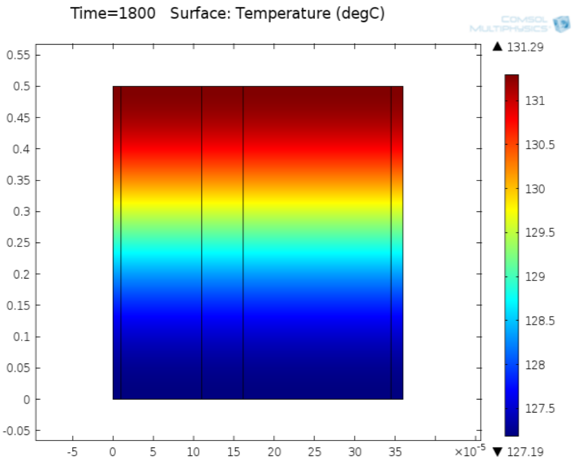

(a) 100% recovery

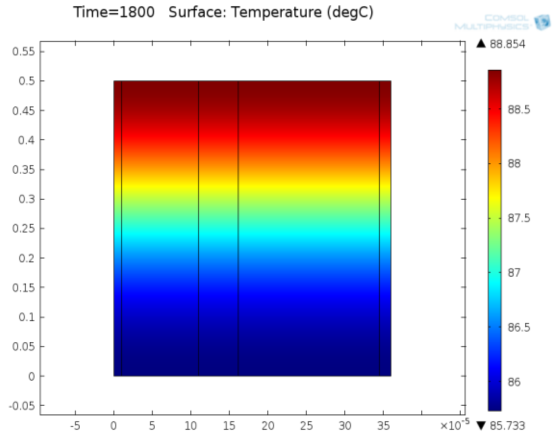

(b) 60% recovery

Figure 9 Temperature variation for recover of regenerative braking energy

Results show considerably higher cell temperature with increased percentage of recovered regenerative energy. For example, the maximum cell temperature is around 88°C for the case 60 % recovery as compared to 130°C for the case of 100 % recovery. For both cases the cell is considerably higher in temperature at the top section where negative and positive terminals are located, and where heat generation due to charge transport and ohmic heating is expected to be high. An extensive cooling scheme is required to keep the cell temperature with a reasonable temperature range for sustained battery kinetics and reactions and optimum cell operation, and for safe operation to avoid so-called thermal run-away of the battery. From the above case, it is clear that 60% recovery is more practical and compared to 100% case.

In order to demonstrate the effect of temperature on the cell performance, a cooling condition is applied to the top and bottom of the battery and the performance is analyzed for voltage and temperature distribution. The cooling effect is produced with the convective boundary condition at the top and the bottom of the cell. The value of the heat transfer coefficient is chosen to be h = 300W/m^{2}K, which is a representative value of natural convection cooling. Comparative results with the adiabatic case are also discussed next.

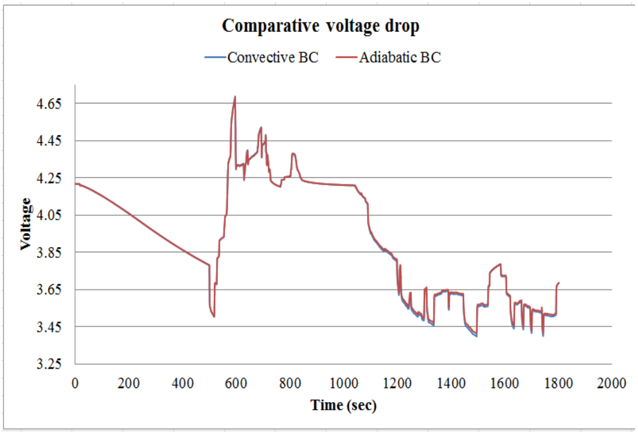

Figure 10 Comparative drop in voltage for 100% and 60%

Figure 10 shows the variation in cell voltage during operation of the load cycle considering two cases: adiabatic and natural convection cooling. A small drop in cell voltage of 0.017 V is noticed for the case of convective cooling. However, the effect on cell temperature is considerably stronger. Average cell temperatures are presented in the Figure 11. In the case of convective cooling the temperature dropped to 73 ºC compared to 87 ºC in adiabatic case. This shows that the thermal runaway of the battery can be controlled based on the proper thermal management.

The effect on overall temperature leads to the analysis of the battery cell for more reduction in temperature and foresee the performance of the battery. The sides of the battery are maintained adiabatic, and to restrict the temperature rise a convective boundary condition is applied at the top and the bottom, In the above discussed cases it is observed that the major temperature rise is at the top so major heat is removed from top and for uniform distribution of temperature bottom is also made convective. The heat transfer coefficient considered for this case is 1200 W/m^2K. This condition has been incorporated in the model. Its effects on the performance of the battery are analyzed based on voltage, salt concentration, overall temperature, and heat generation.

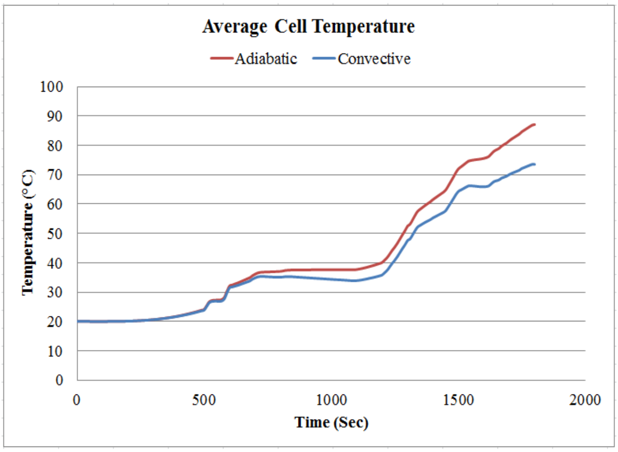

Figure 11 Average cell temperature for convective and adiabatic case

Under the convective condition, the voltage drop is similar to the adiabatic condition. In the open circuit the losses are occurring at 800 seconds to 1100 seconds, and the voltage tries to recover during this phase of 1550 seconds to 1650 seconds. During charging of the battery, the cell has been overcharged due to this rise in voltage to 4.4V. At the first open circuit, the voltage drops from 4.4V to 4.2V. In the discharge phase before the second open circuit, the voltage drops below 3.5V, so the recovery of the voltage takes place, and the rise in the voltage is observed due to overcoming of the ohmic losses and the concentration losses.

The load cycle is further analyzed for the salt concentration, temperature, and heat generation. The lithium concentration variations in solid and liquid phases are presented in Figure 12.

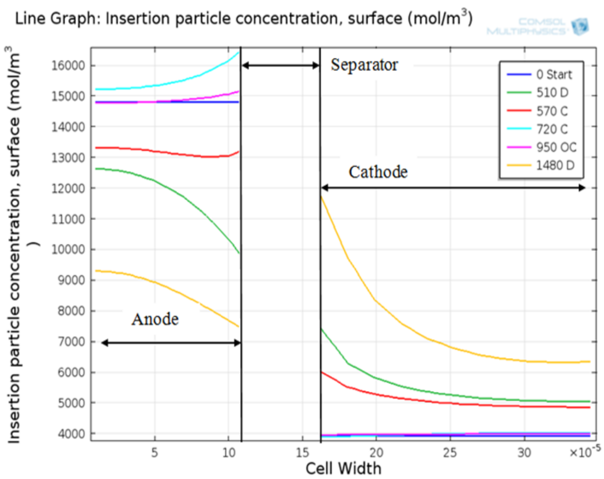

(a) Lithium concentration in solid phase

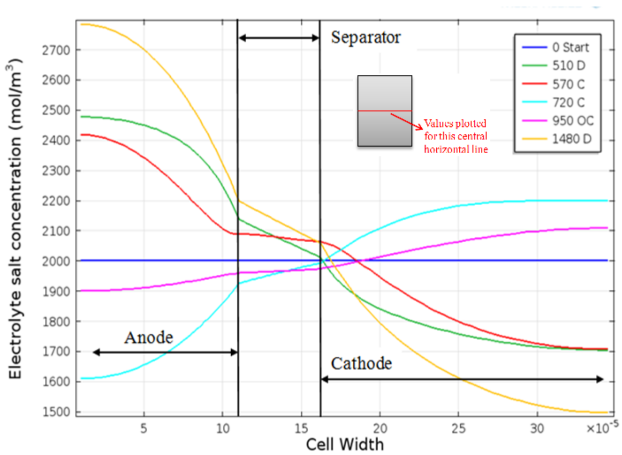

(b) Lithium concentration in liquid phase

Figure 12 Variation lithium concentration distributions during the load cycle

The load cycle is applied to the model, and the convective boundary condition is applied at the top and bottom of the cell. The value of the heat transfer coefficient is 1200 W/m^2 – K. This condition is applied to maintain the internal temperature at a lower value than the adiabatic case.

As we can see that, there is considerable variation in lithium concentration in the electrode layers as the reaction proceeds. As the discharge reaction precedes, lithium ion concentration decreases in the solid phase on the left side of the negative electrode and increases the concentration with the liquid phase. The concentration gradient results in transport of lithium ion towards the positive electrode through the electrolyte. As the discharge continues, the solid phase concentration increases with the positive electrode. The process reverses as the load cycle moves into the region of charging.

The diffusion during the initial 1100 seconds of the load cycle is like the diffusion in the adiabatic case. When the load cycle progresses beyond 1100 seconds the diffusion of the salt is faster. Thus, at the 1480th second the lithium in the liquid phase is greater compared to that in the adiabatic case.

Heat generation in the cell during the convective condition is observed. The maximum amount of heat was generated during charging. The main component of heat contributing to overall heat generation and the temperature rise is the ohmic heat and displayed in Figure 13. More heat is generated with the convective boundary condition. These results follow analysis on the constant load cycle. The trend followed is the similar, and the total heat generated with the convective condition is 4.30 x 10^8 W/m in contrast to the adiabatic condition, 4.06 x 10^8 W/m. Thus, the increase in heat generation is 5.91%.

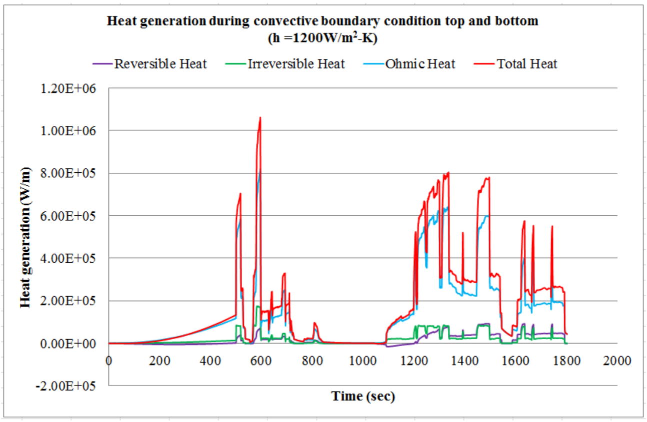

Figure 13 Heat generating components of battery along the complete load cycle

The contour plots in Figure 14 shows the variation of the temperature with respect to load cycle at different time steps.

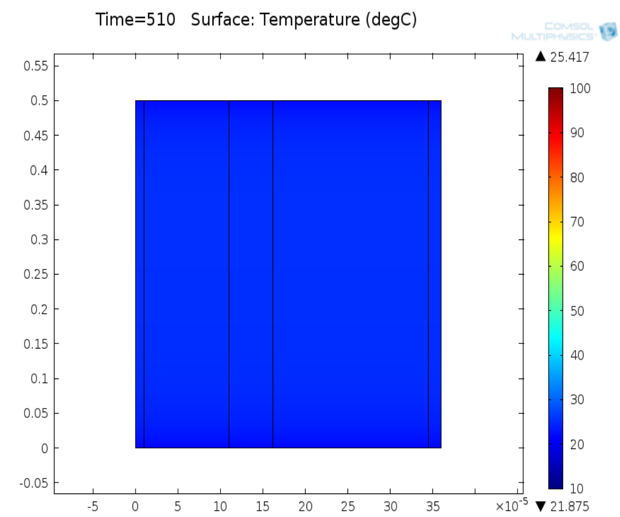

(a) Time = 510

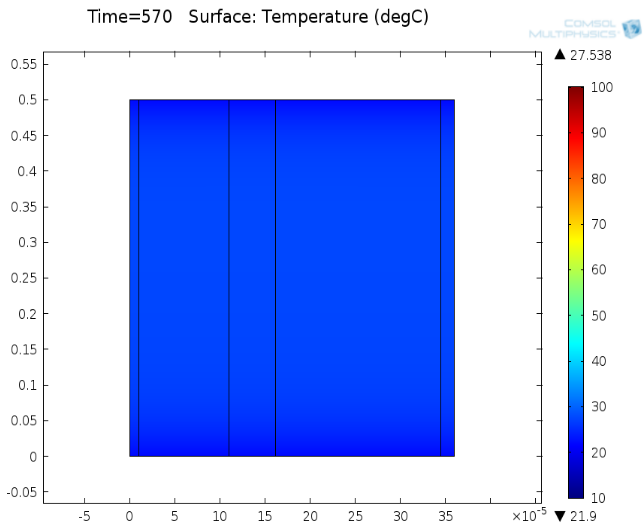

(b) Time = 570

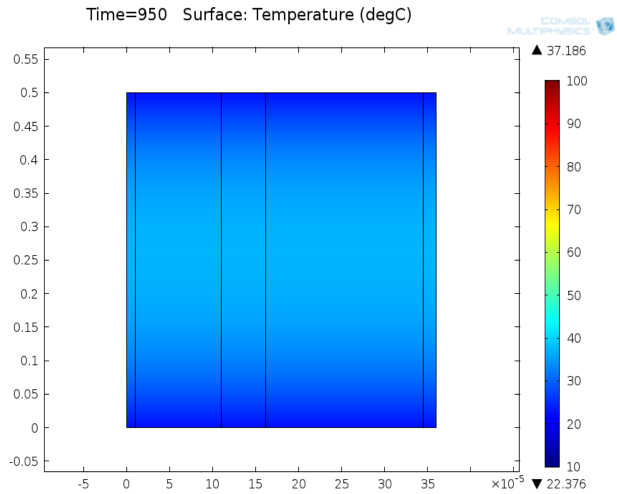

(c) Time = 950

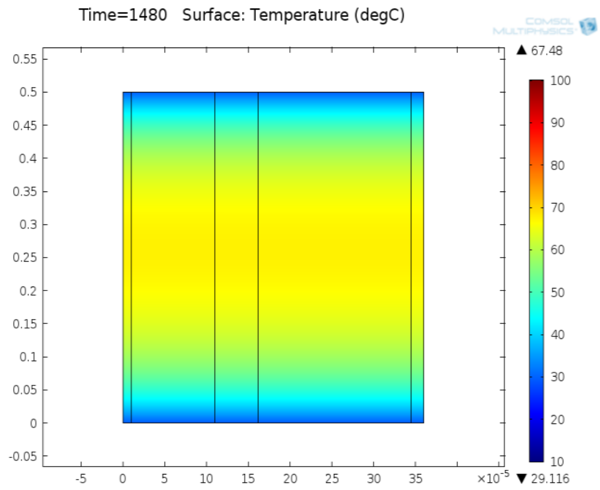

(d) Time = 1480

Figure 14 Temperature contour plots

Due to convective cooling, the top and bottom section of the cell remain cooler than the mid-section of the cell as it clearly visible in Figure 14c and 14d as load cycle proceeds.

Figure 15 shows variation in average cell temperature as well as temperature at the top and bottom sections of the cell with increase in time. The initial rate of increase in temperature is lesser compared to that in the adiabatic case and the temperature is also controlled in the later stage. After charging during the 570th second, the temperature rise is slowly because of slow down of process and constant cooling. During open circuit average temperature reduces by significant amount and can be observed in the figure. Finally, during the continuous discharge process the temperature rises sharply. Compared to the adiabatic condition the overall decrease in central temperature is from 87ºC to 67ºC.

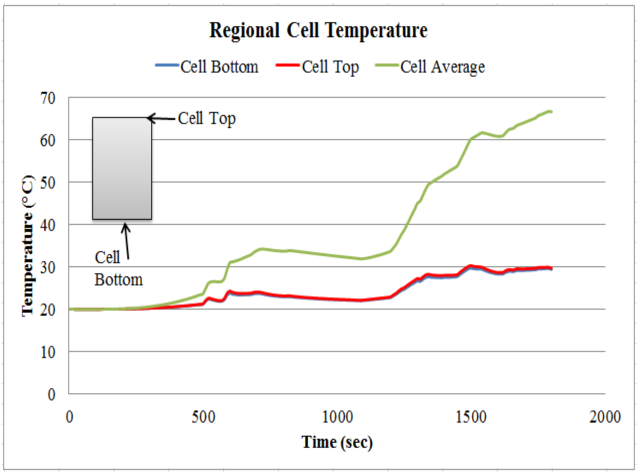

Figure 15. Regional cell temperature during convective condition

VI. Conclusion

A feasibility analysis concludes that a significant fraction of energy lost during dynamic braking is recoverable by regenerative braking. The Battery Energy Storage System is suitable to store the maximum available regenerative braking for the analyzed duty cycle. The volume of the fuel tank for the 2500Hp locomotive is nearly equal to 350 ft^3 and the volume of BESS is nearly the same. This shows the reduction in fuel consumptions; reduce pollution emission, and potential reduction in fuel tank size. Battery simulation analysis shows considerable increase in temperature of the cell with increased percentage of regenerative energy recovered and with time during the engine load cycle involving high peak discharging and discharging. The temperature is better controlled in with effective convective cooling of the cell. The overall temperature rise in case of adiabatic condition was 87.6ºC compared to 67.48ºC for the convective boundary condition considered. The heat generation is more in the case of convective boundary condition case due to enhance battery reactions compared to adiabatic boundary condition, but the battery performance is better.

VII. Acknowledgment

The authors would like to acknowledge support by Dr. Promod Vohra and Dr. Cliff Mirman, College of Engineering and Engineering Technology of Northern Illinois University (NIU).

The work is supported by U.S. Department of Energy under Grant No: DE-EE0003975.

REFERENCES

[1] Mattson J., Thesis topic "Use of Alternative Fuels and Hybrid Vehicles by Small Urban and Rural Transit Systems," pp. 1-10, 2012.

[2] Miller A. R., Peters J., Smith B. E., Velev O.A., "Analysis of fuel cell hybrid locomotives," Journal of Power Sources Volume 157, Issue 2, pp. 855–861, 2006.

[3] Electric locomotive, Retrieved on 20th May http://en.wikipedia.org/wiki/Electric_locomotive, May 2012.

[4] Jalaj Bidawai, Pradip Majumdar, David Schroeder and Kilaparti Rao, Electrochemical and Thermal Run away analysis of Lithium-Ion Battery for Hybrid Locomotive, proceedings of the 2012 ASME Summer Heat Transfer Conference, July 2012.

[5] Nielson G., A. Emadi "Hybrid energy storage systems for high-performance hybrid electric vehicles," Vehicle Power and Propulsion Conference (VPPC), IEEE, Pages 1-6, 2011.

[6] Pedram M., N. Chang, Y. Kim, and Y. Wang, "Hybrid Electrical Energy Storage Systems" ISLPED'10 Proceedings of the 16th ACM/IEEE international symposium on Low power electronics and design, pp. 363-368, 2010.

[7] Ribeiro P. F., B K Johnson, M L Crow, A Arsoy, Y Li, "Energy storage systems for advanced power applications," Proceedings of the IEEE, Volume: 89, Issue: 12, pp. 1744-1756, 2001.

[8] Battery _(electricity), Retrieved on 20th May 2012, http://en.wikipedia.org/wiki/Battery_(electricity), 2012.

[9] Revankar, S and P. Majumdar, Fuel Cells: Principles, Design and Analysis, CRC Press -Taylor & Francis Group, 2014.

[10] Wakihara M., O.Yamamoto, "Lithium-ion batteries: fundamentals and performance," John Wiley & Sons, Inc, USA, pp. 1-25, 1998.

[11] Chan H.L., A New Battery Model for use with Battery Energy Storage Systems and Electric Vehicles Power Systems, Power Engineering Society Winter Meeting, IEEE, vol.1, pp. 470 – 475, 2000.

[12] Cody J., Ö. Göl, Z. Nedic, A. Nafalski, A. Mohtar University of South Australia, (2009), Zeszyty Problemowe – Maszyny Elektryczn, pp. 113-118, 2009.

[13] GATES ENERGY PRODUCTS., "Rechargeable Batteries Applications Handbook," Boston: Butterworth-Heinemann, pp. 271 – 281, 1998.

[14] Neves P. and J. Afonso, "Traction system for electric vehicles using a variable frequency. three-phase induction motor driver with regenerative braking," Proceedings of the International Conference on Hands on Science, 2006.

[15] Narayan R., B. Viswanathan, "Chemical and Electrochemical Energy Systems,", Sangam Books Ltd, pp. 60-80, 1998.

[16] Walter S., Bruno, "Advances in Lithium-Ion Batteries," Publisher: Springer US, DOI: 10.1007/0-306-47508-1_1, pp. 1-5, 2002.

[17] Ghosh D., K. King, B. Schwemmin, Dzho, "Full Hybrid Electrical Vehicle Battery Pack System Design, CFD Simulation and Testing," SAE Technical Paper 2010-01-1080, DOI: 10.4271/2010-01-1080, 2010.

[18] Pesaran A., "Battery Thermal Management in EVs and HEVs: Issues and Solutions," Advanced Automotive Battery Conference Las Vegas, Nevada, Volume: 43 Issue: 5, pp. 34–49, 2001.

[19] Andrew Arendas, Pradip Majumdar, S. Rao Kilaparti and David Schroeder Experimental Investigation of the Thermal Characteristics of Li-Ion Battery for Use in Hybrid Locomotives, ASME Journal of Thermal Science and Engineering Application, 2013.

[20]. Duvall M.S., "Battery Evaluation for Plug-In Hybrid Electric Vehicles" Vehicle Power and Propulsion," IEEE Conference, DOI: 10.1109/VPPC.2005.1554580, pp. 338-343, 2005.

[21] Valence Batteries Technology, http://www.valence.com/sites/default/files/images/XP_Module_Datasheet__1.pdf, 2011, Retrieved on 20th May 2012.

[22] Locomotive size comparison http://en.wikipedia.org/wiki/EMD_SD35, http://thecrhs.org/Information/E8-Technical-Information.